



STEADY-STATE CHARACTERISTICS ANALYSIS OF DEEP-SEA RUNNING MECHANISM WITH PLANETARY GEAR WHEEL BASED ON ARTICULATED STEERING RADIUS

Ya-Li Feng

Department of Vehicle Engineering, Civil and Environmental Engineering School, University of Science and Technology Beijing, Beijing 100083, China., ylfeng126@126.com

Yi-Ting Kang

Department of Vehicle Engineering, Civil and Environmental Engineering School, University of Science and Technology Beijing, Beijing 100083, China.

Wen-Ming Zhang

Department of Vehicle Engineering, Civil and Environmental Engineering School, University of Science and Technology Beijing, Beijing 100083, China.

Jie Zhang

Department of Vehicle Engineering, Civil and Environmental Engineering School, University of Science and Technology Beijing, Beijing 100083, China.

Follow this and additional works at: <https://jmstt.ntou.edu.tw/journal>



Part of the [Electrical and Computer Engineering Commons](#)

Recommended Citation

Feng, Ya-Li; Kang, Yi-Ting; Zhang, Wen-Ming; and Zhang, Jie (2010) "STEADY-STATE CHARACTERISTICS ANALYSIS OF DEEP-SEA RUNNING MECHANISM WITH PLANETARY GEAR WHEEL BASED ON ARTICULATED STEERING RADIUS," *Journal of Marine Science and Technology*. Vol. 18: Iss. 5, Article 20.

DOI: 10.51400/2709-6998.1934

Available at: <https://jmstt.ntou.edu.tw/journal/vol18/iss5/20>

This Research Article is brought to you for free and open access by Journal of Marine Science and Technology. It has been accepted for inclusion in Journal of Marine Science and Technology by an authorized editor of Journal of Marine Science and Technology.

STEADY-STATE CHARACTERISTICS ANALYSIS OF DEEP-SEA RUNNING MECHANISM WITH PLANETARY GEAR WHEEL BASED ON ARTICULATED STEERING RADIUS

Ya-Li Feng*, Yi-Ting Kang*, Wen-Ming Zhang*, and Jie Zhang*

Key words: planetary gear train, steering radius, steady-state characteristic, simulation analysis.

ABSTRACT

Steady-state characteristics analysis for the deep-sea running mechanism with planetary gear train which is designed to adapt to complex terrain in the deep-sea hydrothermal sulfide and rich-cobalt incrustation survey area is based on articulated steering radius. The articulated steering radius formula of the deep-sea running mechanism is derived from the geometric relationship, considering the wheel side slip angle. Based on the formula, three types of steering steady-state characteristic analysis, understeer, neutral steer and oversteer, are made for the mechanism. Steering simulation analysis of the running mechanism with planetary gear is conducted in ADAMS software with different speed. In the process of steering, the side slip angle increases first, then gradually decreases and finally tends to be stable. The side slip angle of the front wheels is greater than that of the rear wheels. While the speed of steering turns to be faster, wheel side slip angle and steering radius increase. The mechanism is understeer, and performs good handling stability characteristic.

I. INTRODUCTION

It is a prevailing field of research about development and utilization about deep-sea hydrothermal sulfide and rich-cobalt incrustation resources [4]. The essential part of the mining technique is concentrated on walking [3].

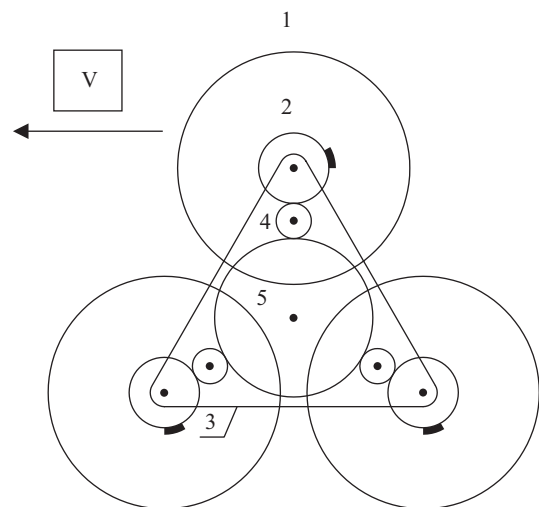
The average depth of the rich-cobalt incrustation and hydrothermal sulfide survey area is about 4000 meters. It includes ocean ridge, seamounts, sea basin and other geological units [8]. The sea-floor is interlaced of rock, sand and mud, of which the compressive strength is 0.08-68.2 Mpa [10], and

terrain grade is 5-35° [6]. Conventional walking mechanisms always turn out to be incompetent when confronting this terrain of multivariate substrate, such as wheeled model, track, legged and complex ways [2].

Planetary gear wheel walking mechanism has a strong adaptability to overcome obstacle [1]. The articulated frame performs good steady-state characteristic, and enhances the stability of the mechanism [7].

II. STRUCTURE AND OPERATING PRINCIPLE OF PLANETARY WHEELS

The structure of planetary gear train is shown in Fig. 1. The center gear 5 drives transition gear 4 and driving gear 2. And the driving gear 2 is fixed with wheel 1, which leads wheel 1 to rotate. According to different forces applied to the wheel 1 by ground, the running mechanism turns into the fixed wheels or the planetary wheels pattern. When it walks on flat ground, two wheels below are restrained by ground, and the planetary



1. wheels; 2. driving gear; 3. planetary wheel carrier; 4. transition gear; 5. center gear

Fig. 1. The structure of planetary gear train of running mechanism.

Paper submitted 08/24/09; revised 11/16/09; accepted 03/22/10. Author for correspondence: Ya-Li Feng (e-mail: ylfeng126@126.com).

*Department of Vehicle Engineering, Civil and Environmental Engineering School, University of Science and Technology Beijing, Beijing 100083, China.

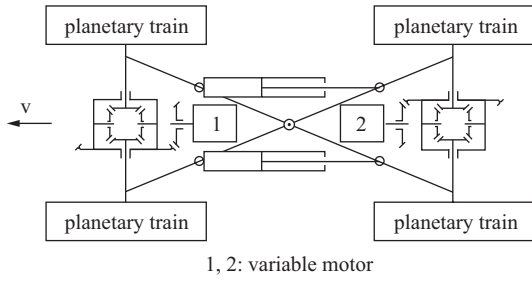


Fig. 2. The design of running mechanism with planetary gear wheel.

wheel carrier 3 can only transit horizontally along with the road [13], so it's the fixed-spindle wheel pattern. When the front wheel encounters obstacles and stop, according to the relationship of the differential gear transmission ratio, it turns into planetary gear train, in which condition planetary wheel carrier 3 with the other two wheels rotate around the central axis of the wheel which has touched the barrier to achieve the function of overcoming obstacles [12]. Because of the connection of the three planetary wheels and a shaft, they are defined as a whole wheel in the steady-state steering performance analysis.

III. THE GEOMETRIC DESCRIPTION OF STEADY STEERING

1. Running Mechanism

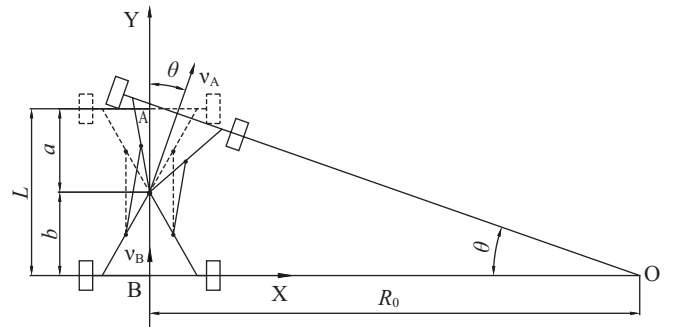
As shown in Fig. 2, the chassis of such running mechanism is made up of front axle and rear axle. There are four sets of planetary gear train, each of which is driven by the running mechanism's wheel. As the fixed-spindle gear train, two wheels are on flat ground, which is equal to 8 × 8 wheels drive. While surmounting obstacles, they evolve into the planetary gear train. The planetary gear carrier rotates to overcome the barrier.

2. Articulated Steering Radius at Low Speeds

To change direction, the pressure oil, produced by the hydraulic system through application valve, drives steering cylinder piston rod to move telescopically [5]. They are located on both the front and rear frame. So, as shown in Fig. 1, either of the frames turns a certain angle, to achieve turning function. Running mechanism makes circular movement around the center of intersection point of front wheel's vertical line and rear wheel's. The distance between the intersectional point and the centerline of the frame is the steering radius as the geometric relationship shown in Fig. 3.

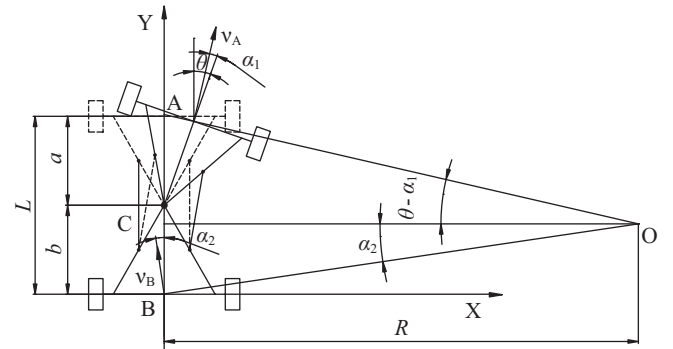
$$\tan \theta = \frac{\frac{a}{\cos \theta} + b}{R_0}$$

$$R_0 = \frac{\frac{a}{\cos \theta} + b}{\tan \theta} \quad (1)$$



O: steering center; R_0 : steering radius; L : wheelbase; θ : average steering angle of the front wheel; a : distance between the front axle and the articulated point; b : distance between the rear axle and the articulated point

Fig. 3. The schematic of running mechanism working in low speed.



O: steering center; R : steering radius; L : Wheelbase; θ : average steering angle of the front wheels; a : distance between the front axle and the articulated point; b : distance between the rear axle and the articulated point; v_A : the speed of the front axle; v_B : the speed of the rear axle; α_1 : the side slip angle of the front wheel; α_2 : the side slip angle of the rear wheel; A: the center of the front axle; B: the center of the rear axle; C: the articulated point

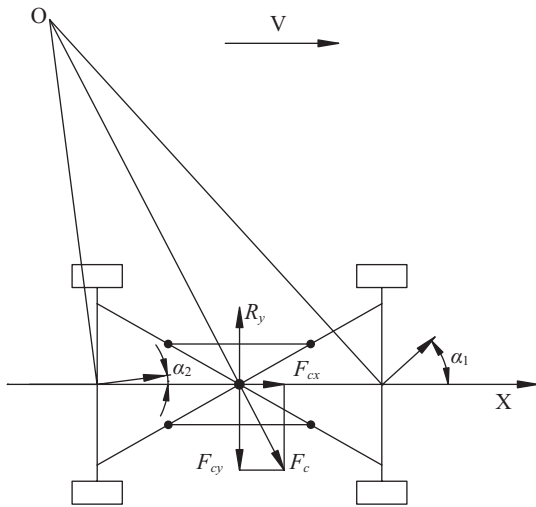
Fig. 4. The schematic of running mechanism considering the side slip angle.

3. The Steering Radius Considering the Side Slip Angle

When a vehicle is negotiating a turn, to balance the centrifugal force, the tires must develop an appropriate side force [11]. A side force acting on a tire produces a side slip angle. Particularly when the speed is higher, the angle is larger. Figure 4 shows that after the front wheels turn a certain angle, the side slip angle also need to be taken into account when analyzing the front wheel speed and the steering radius. According to the geometric relationships of triangle OAC and OBC as shown in Fig. 4:

$$\tan(\theta - \alpha_1) = \frac{\overline{AC}}{R}$$

$$\tan \alpha_2 = \frac{\overline{BC}}{R}$$



α_1 : the side slip angle of the front wheel; α_2 : the side slip angle of the rear wheel; F_c : centrifugal force; F_{cy} : side component force; R_y : side force

Fig. 5. The schematic of running mechanism with understeer characteristic.

$$\begin{aligned} \tan(\theta - \alpha_1) + \tan \alpha_2 &= (\overline{AC}/R) + (\overline{BC}/R) \\ &= \overline{AB}/R \\ &= \frac{a \cos \theta + a \sin \theta \tan(\theta - \alpha_1) + b}{R} \end{aligned}$$

So:

$$R = \frac{a \cos \theta + a \sin \theta \tan(\theta - \alpha_1) + b}{\tan(\theta - \alpha_1) + \tan \alpha_2}$$

Because most articulation joints are located in the center of the running mechanism, $a = b = L/2$, so

$$\begin{aligned} R &= \frac{\cos \theta + a \sin \theta \tan(\theta - \alpha_1) + 1}{\tan(\theta - \alpha_1) + \tan \alpha_2} a \\ &= \frac{\frac{1}{\cos \theta} + 1 + \tan \theta \tan \alpha}{\tan(\theta - \alpha_1 + \alpha_2)[1 - \tan(\theta - \alpha_1) \tan \alpha_2](1 + \tan \theta \tan \alpha_1)} a \end{aligned}$$

Because the value of the side slip angle does not exceed the range from 4° to 5° generally, and the maximum steering angle is between 40° and 42° [15], we can get:

$$\tan \theta \tan \alpha \approx 0, [1 - \tan(\theta - \alpha_1) \tan \alpha_2](1 + \tan \theta \tan \alpha_1) \approx 1$$

$$\text{So: } R = \frac{\frac{1}{\cos \theta} + 1}{\tan[\theta - (\alpha_1 - \alpha_2)]} a \quad (2)$$

Compared (2) with (1), the difference is an extra $(\alpha_1 - \alpha_2)$ in the independent variables of the tangent function of the denominator.

4. The Steering Characteristics Analysis Based on the Steering Radius

According to the difference between α_1 and α_2 , the average side slip angle of the front wheel and the rear one, there are three conditions as following.

If $\alpha_1 = \alpha_2$, $R = R_0$, it is said to be “neutral steer”. For a neutral steer vehicle, when it is accelerated in a constant radius turn, the driver should maintain the same steering wheel position. In other words, the turning radius remains when the vehicle is accelerated with fixed steering wheel. When a neutral steer vehicle originally moving along a straight line is subjected to a side force acting at the center of gravity, equal slip angles will be developed at the front and the rear tires. As a result, the vehicle follows a straight path at an angle to the original.

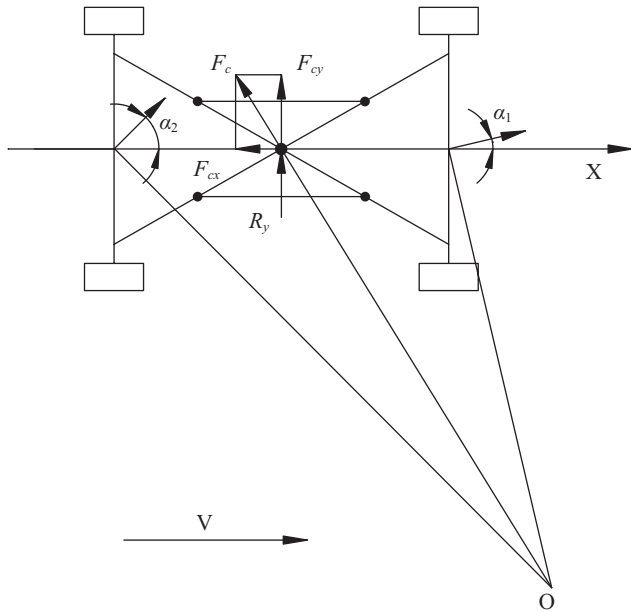
If $\alpha_1 > \alpha_2$, $R > R_0$, it is said to be “understeer”. For an understeer vehicle, when it is accelerated in a constant radius turn, the driver must increase the steering wheel’s angle. In other words, the turning radius increases when the vehicle is accelerated with fixed steering wheel. At the same steering wheel position and vehicle forward speed, the turning radius of an understeer vehicle is larger than that of a neutral steer vehicle. When a side force acts at the center of gravity of understeer vehicle originally moving along a straight line, the front tires will develop a slip angle greater than that of the rear tires. As a result, a yaw motion is initiated, and the vehicle turns to the direction of the side force, as shown in Fig. 5.

If $\alpha_1 < \alpha_2$, $R < R_0$, it is said to be “oversteer”. For an oversteer vehicle, when it is accelerated in a constant radius turn, the driver must decrease the steering wheel’s angle. In other words, the turning radius decreases when the vehicle is accelerated with fixed steering wheel. For the same steering wheel position and vehicle forward speed, the turning radius of an understeer vehicle is smaller than that of a neutral steer vehicle. When a side force acts at the center of gravity of an oversteer vehicle originally moving along a straight line, the front tires will develop a slip angle less than that of the rear tires. As a result, a yaw motion is initiated, and the vehicle turns into the opposite direction of side force, as shown in Fig. 6.

IV. SIMULATION ANALYSIS OF ARTICULATED STEERING

Steering simulation analysis of the running mechanism with planetary gear is conducted in ADAMS software with different speed.

ADAMS is the abbreviation for “Automatic Dynamic Anal-



α_1 : the side slip angle of the front wheel; α_2 : the side slip angle of the rear wheel; F_c : centrifugal force; F_{cy} : side component force; F_{cx} : side force; R_y : side force

Fig. 6. The schematic of running mechanism with oversteer characteristic.

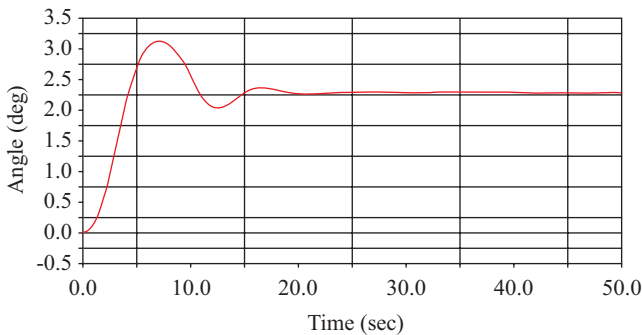


Fig. 7. The change curve of the front wheel's side slip angle.

ysis of Mechanical Systems”. It is a software for virtual prototyping analysis developed by MDI corporation in America.

The structure of running mechanism has been simplified in the process of modeling. The link rod components are used instead of the suspension of running mechanism, wheels and ground are connected by tire force, driving force is set on the sun gear of the planetary gear train, and the articulation joint is replaced by two superposed revolute joint of orthogonal Z-axis [14]. The main parameters of model are as follows: speed 0~1 m/s, wheel radius 0.34 m, axle base 2 m, wheel track 1.5 m, and weight 6 t [9].

At 0 sec, steering cylinders start working. At 10 sec, they arrive at the scheduled position, which means that the running mechanism reach the scheduled steering angle. The main conditions of simulation are as follows: with the steering angle of

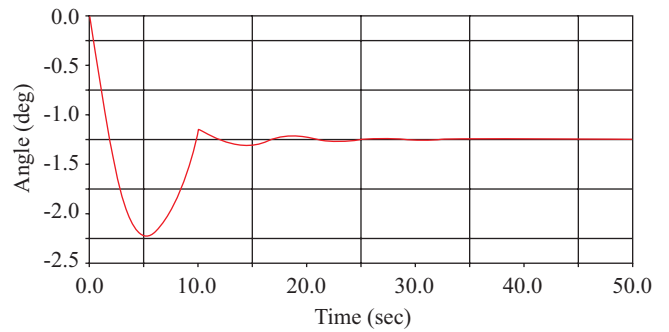


Fig. 8. The change curve of the rear wheel's side slip angle.

Table 1. The steady side slip angle of planetary and the steering radius.

Vehicle speed m/s	0.05	0.1	0.15	0.2	0.25	0.3
Front wheel's side slip angle °	0.191	0.895	1.586	1.907	2.482	3.115
Rear wheel's side slip angle °	-0.130	-0.752	-1.384	-1.523	-1.854	-2.140
Steering radius m	4.992	5.336	5.722	5.868	6.176	6.519

23°, running mechanism steers in different speed. The research is about its steering performance and the change of the side slip angle in the process of steering. To set a sample, a series of the curves are given below. They are the stability value of the side slip angle of planetary gear wheels in the simulation of running mechanism's steering and the change curve of the side slip angle of wheels, at the speed of 0.2 m/s.

Figure 7 is the change curve of the front wheel's side slip angle, and Fig. 8 is that of the rear. It is shown that, during the turning, the side slip angle of the wheel increases continuously, and reaches a peak. After the steering angle of front wheel and rear wheel reach a scheduled value, the side slip angle of the wheel reduces continuously, and basically remains at the same value at last. As shown in Fig. 8, the slip angle of rear wheel changes abruptly at 10 sec, and then tends to be stable. Because at 10 sec, the steering cylinder arrive at the scheduled position, which means the steering angle of rear wheel has reached the scheduled value 23°. According to Table 1, when the speed changes from small to large with a constant steering angle, the side slip angle of both the front and rear wheel grow larger continuously. And the front wheels' side slip angle is larger. The steering radius also increases. The running mechanism is understeer and has good handling stability.

V. CONCLUSIONS

According to the geometrical relationship, the articulated steering radius formula of deep-sea running mechanism with planetary gear wheel is derived considering the wheel side slip angle. When the front wheel is turning a certain angle, if the value of $(\alpha_1 - \alpha_2)$ increases, and the steering radius increases

either, the running mechanism has an oversteer characteristic. Otherwise, if the value of $(\alpha_1 - \alpha_2)$ reduces, and the steering radius decreases, it is understeer. If the value of $(\alpha_1 - \alpha_2)$ is zero, the steering radius remains the same during turning, it is neutral steer.

The analysis for the deep-sea running mechanism with planetary gear wheel which can adapt to complex terrain in the deep-sea hydrothermal sulfide and rich-cobalt incrustation survey area, derived the articulated steering radius formula on the basis of three types of steering steady-state characteristic analysis, understeer, neutral steer and oversteer. The steering steady-state characteristic of running mechanism depends on the side slip angle.

The results of ADAMS simulation analysis show that, with the increase of the steering speed, the wheel side slip angle of running mechanism and the steering radius increase. It is understeer. The result of simulation satisfies the theoretical analysis results very well. To draw a conclusion, the deep-sea running mechanism with planetary gear wheel performs good handling stability characteristic.

REFERENCES

1. Bapna, D., Rollins, E., Murphy, J., Maimone, E., Whittaker, W., and Wettergreen, D., "The Atacama desert trek: Outcome," *Proceedings of IEEE International Conference on Robotics and Automation*, Detroit, MI, USA, pp. 597-604 (1998).
2. Bo, Y. Y., Liu, G. H., Shi, C. X., and Wang, J. C., "Study on dead reckoning for a deep-sea cobalt-rich mining vehicle," *Journal of Zhengzhou University (Engineering Science)*, Vol. 28, No. 1, pp. 12 (2007).
3. Chung, J. S., "Deep-oceanmining: Technologies for manganese nodules and crusts," *International Journal of Offshore and Polar Engineering*, Vol. 6, No. 4, pp. 244 (1996).
4. Feng, Y. L., Li, H. R., and Zhang, W. M., "Future trends of deep sea bed mining technology," *Journal of University of Science and Technology Beijing*, Vol. 6, No. 1, pp. 4-7 (1999).
5. Feng, Y. L., Zhang, W. M., and Feng, F. Z., "Design and strength analysis of a spherical connector for lifting subsystem in deep sea mining system," *China Ocean Engineering*, Vol. 20, No. 4, pp. 605-613 (2006).
6. Glasby, G. P., "Deep seabed mining: Past failures and future prospects," *Marine Georesources and Geotechnology*, Vol. 20, pp. 165-169 (2002).
7. Huang, Z. H., Liu, S. J., and Xie, Y., "Obstacle performance of cobalt-enriching crust wheeled mining vehicle," *Computer Simulation*, Vol. 23, No. 5, pp. 200 (2000).
8. KORDI, "Exploration for manganese crusts in the southwestern pacific," *Annual Report*, pp. 102-112 (2002).
9. Masuda, Y., "Crust mining plans of the Japan Resources Association," *Marine Mining*, Vol. 10, pp. 95 (1991).
10. Moon, J. W., "Current state and future prospect of Korean activities on the seafloor sulfides and cobalt-rich crusts," *International Symposium on New Deep Seabed Mineral Resources Development Policy*, Ansan, Korea, pp. 203-208 (2004).
11. Nandy, G. C. and Xu, Y. S., "Dynamic model of a gyroscopic wheel," *Proceedings of the IEEE Intenational Conference on Robotics and Automation*, Detroit, MI, USA, pp. 2683 (1998).
12. Qiao, F. B. and Yang, R. Q., "Analysis on the stair climbing ability of six wheeled mobile robot," *Robot*, Vol. 26, No. 4, pp. 301 (2004).
13. Rollins, E., Luntz, J., Foessel, A., Shamah, B., and Whittaker, W., "A demonstration of the transforming chassis," *Proceedings of the IEEE International Conference on Robotics and Automation*, Detroit, MI, USA, pp. 611-617 (1998).
14. Wang, J. J., Li, L., and Chen, J. T., "Research on the performance of a new type of deep-sea all-terrain cobalt-crust mining vehicle based on simulation," *Mechanical Engineering & Automation*, Vol. 23, No. 4, pp. 1 (2007).
15. Yu, Z. S., *Automobile Theories*, China Machine Press, Beijing (2006).